

# Universal geometrical scaling for hadronic interactions

C. Andrés, A. Moscoso, C. Pajares

*Departamento de Física de Partículas and IGFAE, Universidade de Santiago de Compostela, 15782, Santiago de Compostela, Spain*

## Abstract

It is shown that defining a suitable saturation momentum  $Q_s$ , the  $p_T$  distributions of pp and AA collisions for any centrality and energy depend only on  $\tau = p_T^2/Q_s^2$  for  $p_T < Q_s$ . For different projectiles, targets and centralities, the corresponding  $\tau$ -lines present small differences for  $\tau < 1$ . For  $\tau > 1$ , the higher the energy or the larger the size of the participant nuclei, the larger suppression present the respective spectra. The integrated spectrum gives a fraction of the hard multiplicity in the range from 9 % for pp at 0.9 TeV to 2 % for Pb-Pb central collisions at 2.76 TeV.

## 1. Introduction

Recently, it has been shown that in pp collisions the  $p_T$  spectra of charged particles exhibit geometrical scaling [1, 2]. Indeed, the  $p_T$  spectra in pp collisions in the broad range of energies from 0.9 to 7 TeV scale in a single variable  $\tau \equiv p_T^2/Q_s^2$ , where the proton saturation momentum  $Q_s^p$  is given by

$$(Q_s^p)^2 \equiv Q_0^2 \left( \frac{W}{p_T} \right)^\lambda, \quad (1)$$

where  $W = \sqrt{s} \times 10^{-3}$  and  $\lambda = 0.3$ .

In this paper, we study the extension of the geometrical scaling to AA collisions, considering RHIC and LHC energies, different centralities and different nuclei. We will show that the geometrical scaling is valid not only for each collision at fixed centrality separately but also for any centrality for  $\tau < 1$ . On the other hand, integrating the hard spectrum for  $\tau > 1$  we obtain that the hard multiplicity fraction decreases with the size of the participant nuclei as it would be expected from jet quenching.

## 2. The saturation momentum

In order to check the geometrical scaling in AA collisions for any centrality we define the saturation momentum  $Q_s^A$  by

$$(Q_s^A)^2 = (Q_s^p)^2 N_A^{\alpha(s)/2} A^{1/6} \left( \frac{A}{N_A} \right)^{1/3} \quad (2)$$

where

$$\alpha(s) = \frac{1}{3} \left( 1 - \frac{1}{1 + \ln(\sqrt{s/s_0} + 1)} \right). \quad (3)$$

$N_A$  is the number of participant nucleons and  $A$  is the number of nucleons.

We observe that at high energy  $\alpha(s) = 1/3$ . With this value, for  $N_A = A$  we recover the commonly used behaviour of  $Q_s^A$  for central collisions  $(Q_s^A)^2 = (Q_s^p)^2 A^{1/3}$ .

*Email address:* pajares@fpaxp1.usc.es (C. Pajares)

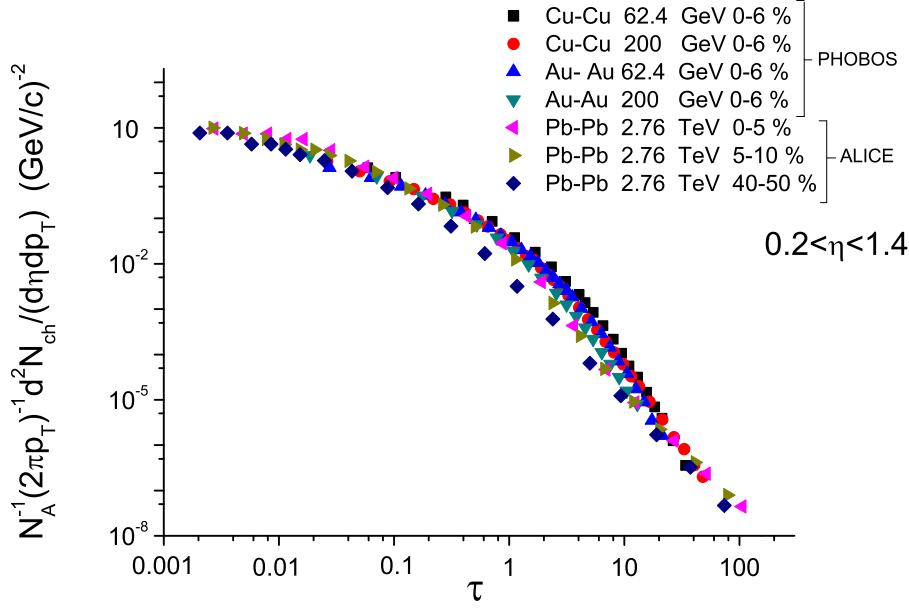


Figure 1: (Colour online.) Charged particle multiplicity per participant at pseudorapidity  $0.2 < \eta < 1.4$  for Au-Au and Cu-Cu central collisions at two RHIC energies 62.4 and 200 GeV [8, 9] and for Pb-Pb collisions at 2.76 TeV [10] plotted as a function of  $\tau$  for  $\lambda = 0.30$ .

The parametrization of equation (2) takes into account the different experimental multiplicity obtained in collisions between different nuclei and same number of participants. Also, it takes into account the well known behaviour of the multiplicity per participant as a function of the number of participants. The detailed shape is taken from the parametrization of references [3, 4] which was used to describe the multiplicities of pp and AA at all centralities, rapidities and energies. The function  $\alpha(s)$  of formula (3) was introduced due to the energy-momentum conservation effects which can explain the different exponent of the power-like energy dependence of the pp and AA multiplicities. In fact, in usual string like or color flux tube models, the number of strings exchanged between the projectile and the target grows with the number of collisions which behaves like  $N_A^{4/3}$ , in such a way that the number of strings exchanged in central AA collisions at a fixed energy  $\sqrt{s}$  is  $A^{4/3} N_s$ , being  $N_s$  the number of strings exchanged in pp. As in AA collisions the available energy is  $A\sqrt{s}$ , at not very high energies there is not enough energy to form such large number of strings and it is expected a suppression of the power  $4/3$  to  $1 + \alpha(s)$ , with  $\alpha(s) \rightarrow 1/3$  at high energy. On the other hand, as the energy of each string is related to the longitudinal phase space that grows like  $\ln s$ , the approach to the asymptotic limit  $1/3$  should be of logarithm type as in formula (3).

The values of the parameters  $\lambda$ ,  $Q_0$  and  $\sqrt{s_0}$  of formulas (2) and (3) are taken from the references [1] and [3], being

$$\lambda = 0.3, \quad Q_0 = 1 \text{ GeV}, \quad \sqrt{s_0} = 245 \text{ GeV}.$$

### 3. Comparison with experimental data (RHIC, LHC)

In Fig. 1, we plot the data  $(N_A 2\pi p_T)^{-1} d^2 N_{ch} / (dp_T d\eta)$  for Cu-Cu 0-6 % central at 62.4 and 200 GeV and Au-Au 0-6 % central at 62.4 and 200 GeV [8, 9] together with Pb-Pb 40-50 %, 5-10 % and 0-5 % at 2.76 TeV [10] as a function of  $\tau$ , in the pseudorapidity range  $0.2 < \eta < 1.4$ . The number of participants used is the mean value corresponding to the given centrality. Experimental data taken from ALICE [10] correspond to a pseudorapidity range including the  $\eta = 0$  region, in which  $dn/d\eta$  is smaller than in the pseudorapidity range considered here. Because of this a 15 % correction was applied to the normalization [4].

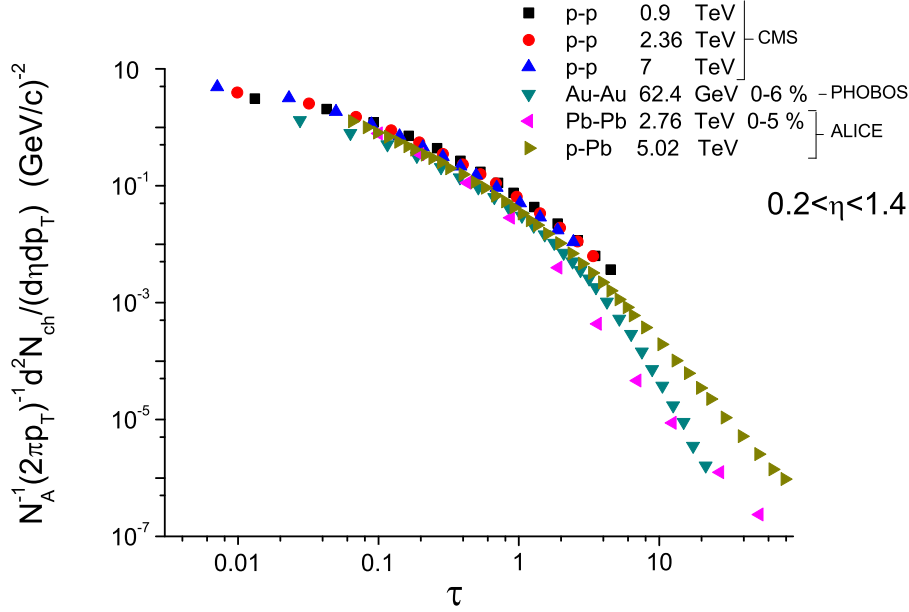


Figure 2: (Colour online.) Charged particle multiplicity per participant at pseudorapidity  $0.2 < \eta < 1.4$  for pp collisions [5–7], Au-Au 0-6 % central collisions at 62.4 GeV [8], Pb-Pb 0-5 % collisions at 2.76 TeV [10] and p-Pb data at 5.02 TeV [11] versus  $\tau$  for  $\lambda = 0.30$ .

It can be seen that Pb-Pb 0-5 % and 5-10 % data points are in the same line for  $\tau < 1$ . Also the Cu-Cu and the Au-Au data points at both energies are approximately in the same curve for  $\tau < 1$ . Only the Pb-Pb 40-50 % points present some departure around 1. For  $\tau > 1$  it is shown a suppression for the heavy nuclei.

In order to see the differences between the different sizes of projectile and target, in Fig. 2 we plot the data for pp collisions at 0.9, 2.36 and 7 TeV [5–7] together with the recent p-Pb data at 5.02 TeV [11], the Au-Au 0-6 % central data at 62.4 GeV [8] and the Pb-Pb 0-5 % data at 2.76 TeV [10] in the pseudorapidity range  $0.2 < \eta < 1.4$ . For the p-Pb data we use  $\langle N_{part} \rangle = 7.9$  such as it is quoted in reference [12].

We observe that the pp data at different energies are in the same line, satisfying geometrical scaling, as it was shown in reference [1]. On the other hand, we observe that the p-Pb, Pb-Pb 0-5 % and Au-Au 0-6 % central data at low  $\tau$  are very close to the pp data of different energies. As far as  $\tau$  becomes larger the difference between these sets of data increases. For  $\tau > 1$  the suppression is larger for Pb-Pb 0-5 % central than for p-Pb, and for the latter there is more suppression than for pp data.

In Fig. 3, we plot together all the previous data to show that for  $\tau < 1$  there are not many differences between them, what does not occur for  $\tau > 1$  which is larger for larger sizes of nuclei.

In order to see the quality of this extended scaling we show in Fig. 4 the ratio of Pb-Pb 0-5 % at 2.76 TeV, Au-Au 0-6 % at 200 GeV, Cu-Cu 0-6% at 62.4 GeV, pPb at 5.02 TeV over Cu-Cu 0-6% at 200 GeV as a function of  $\tau$ . Even for such different projectiles and targets and also in the broad range of energies considered, we observe an approximate scaling at low  $\tau$ . Notice that for  $\tau < 1$  the data extend over three orders of magnitude. Excluding the Cu-Cu data, the ratios vary between 0.7 and 1.3 in the range  $0.2 < \tau < 1$ . The violation of the scaling is clear for  $\tau > 1$ , showing a higher suppression for heavier nuclei. The hierarchy of the scaling violations for  $\tau > 1$  agree with the expected suppression due to jet quenching.

Based on this approximate scaling, we can compute the multiplicity of soft and hard particles per participant, defining soft particles as those with  $p_T < Q_s$  and hard as those with  $p_T > Q_s$ . In fact,

$$\frac{1}{N_A} \frac{dN_{ch}^{soft}}{d\eta} = \frac{1}{N_A} \int_0^{Q_s^2} dp_T^2 \frac{dN_{ch}^2}{d\eta dp_T^2} = \frac{1}{N_A} \int_0^{Q_s^2} dp_T^2 \frac{1}{Q_0^2} F(\tau) \quad (4)$$

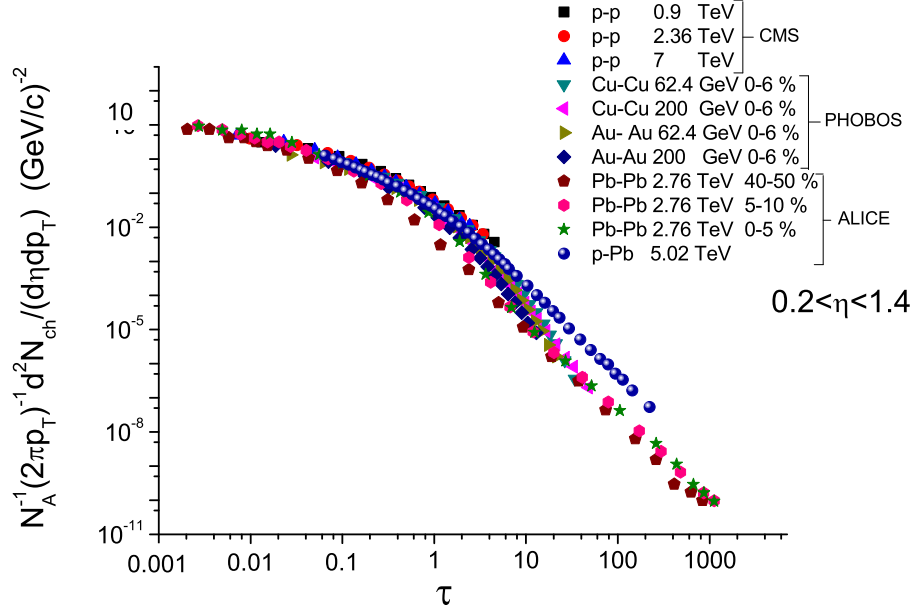


Figure 3: (Colour online.) Charged particle multiplicity per participant in the pseudorapidity range  $0.2 < \eta < 1.4$  for all the heavy ion collisions considered plotted as a function of  $\tau$  for  $\lambda = 0.30$ .

and with the change of variables

$$\frac{dp_T^2}{Q_0^2} = \frac{2}{2+\lambda} \left( \frac{W}{Q_0} \right)^{\frac{2\lambda}{2+\lambda}} \tau^{-\frac{\lambda}{2+\lambda}} N_A^{\alpha(s)/2} A^{1/6} \left( \frac{A}{N_A} \right)^{1/3} d\tau, \quad (5)$$

the fraction of soft and hard multiplicities over the total multiplicity results

$$R_s \equiv \frac{dN_{ch}^{soft}/d\eta}{dN_{ch}^{tot}/d\eta} = \frac{\int_0^1 d\tau \tau^{-\frac{\lambda}{2+\lambda}} F(\tau)}{\int_0^\infty d\tau \tau^{-\frac{\lambda}{2+\lambda}} F(\tau)}, \quad R_h \equiv \frac{dN_{ch}^{hard}/d\eta}{dN_{ch}^{tot}/d\eta} = \frac{\int_1^\infty d\tau \tau^{-\frac{\lambda}{2+\lambda}} F(\tau)}{\int_0^\infty d\tau \tau^{-\frac{\lambda}{2+\lambda}} F(\tau)} \quad (6)$$

In Table 1 we present the results for the fractions of soft and hard multiplicities for the centralities, energies and collisions considered. In order to do the integration in (6), we do first a fit to each  $p_T$ -distribution separately, that afterwards is integrated.

We observe that the hard fraction decreases slowly with energy and that it also decreases with the size of the participant nuclei. In the case of pp collisions the dependence of the energy is very weak, varying from 9 % to 8 % in the broad range 0.9-7 TeV. However, we observe larger differences between Au-Au 0-6 % central at 62.4 GeV, whose hard fraction is 7 %, and Pb-Pb 0-5 % at 2.76 TeV, which is 2 %. For Pb-Pb at 2.76 TeV the hard fraction is the same for peripheral (40-50 %) than for central (0-5 %).

#### 4. Conclusions

Usually it is thought that as the energy or the size of the participant nuclei increases, the weight of the hard collisions increases and correspondingly the weight of the hard multiplicity. We observe the opposite with our definition of hard and soft collisions. This result was also pointed out by the ALICE collaboration data of the sphericity as a function of the energy and the change multiplicity in pp collisions at 0.9, 2.36 and 7 TeV [13, 14]. The sphericity measures the jet activity, in such a way that one event with dijet back to back implies sphericity zero. On the contrary,

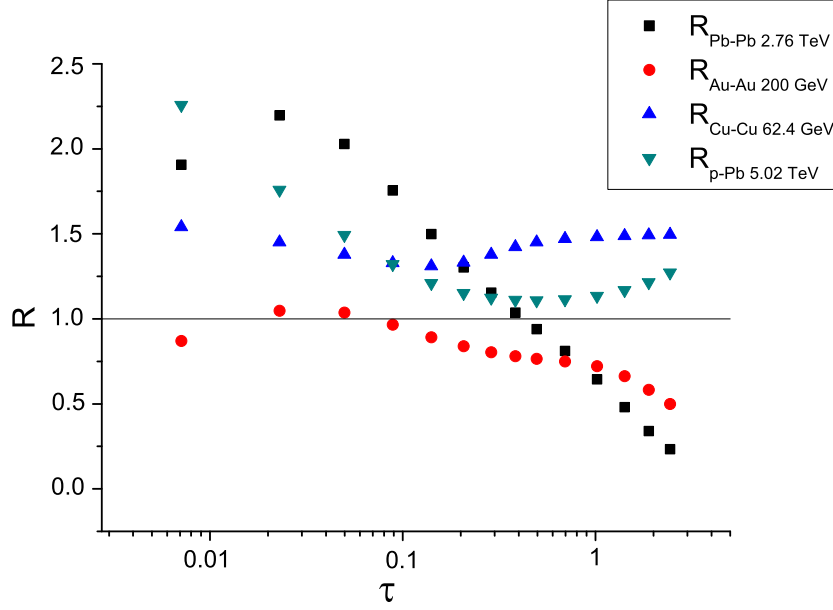


Figure 4: (Colour online.) Ratio of Pb-Pb 0-5 % at 2.76 TeV [10], Au-Au 0-6 % central at 200 GeV [8], Cu-Cu 0-6% central at 62.4 GeV [9], pPb at 5.02 TeV [11] over Cu-Cu 0-6% at 200 GeV [9] in terms of  $\tau$ .

an event where all the produced particles are distributed isotropically in phase space implies sphericity one. Most of the Monte-Carlo codes (Pythia 8, Perugia-0, Phojet, Atlas-CSC) predict a decreasing of the sphericity with energy and charged multiplicity whereas the data show the opposite trend. In the color glass condensate model [15, 16] the further the saturation momentum grows with the energy and the number of participants, the smaller room exists for hard collisions. This also happens in the framework of percolation strings [17, 18] where the area covered by strings increases with energy and size of the nuclei leaving less room for hard scatterings.

Let us mention that the scaling found is naturally incorporated in the color glass condensate [15, 16] where the  $p_T$  spectrum depends only on  $p_T^2/Q_s^2$ . In the model of percolation of strings [17, 18] also is obtained an scaling law for the  $p_T$  dependence. Now the role of  $Q_s^2$  is played by  $\sqrt{\eta'}$  where  $\eta'$  is the string density [19]. Indeed the parametrization (2) has its origin in the parametrization of  $\sqrt{\eta'}$  [3].

In conclusion, we have shown that the geometrical scaling seen previously in pp collisions can be extended to AA

	Energy (TeV)	Centrality	$R_s$	$R_h$
p-p	0.9	minb	0.91	0.09
p-p	2.36	minb	0.90	0.10
p-p	7	minb	0.92	0.08
p-Pb	5.02	minb	0.93	0.07
Cu-Cu	0.0624	0-6 %	0.93	0.07
Cu-Cu	0.2	0-6 %	0.94	0.06
Au-Au	0.0624	0-6 %	0.93	0.07
Au-Au	0.2	0-6 %	0.96	0.04
Pb-Pb	2.76	40-50 %	0.98	0.02
Pb-Pb	2.76	0-5 %	0.98	0.02

Table 1: Values of the fractions of soft and hard multiplicities for different nuclei, centralities and energies.

collisions, being satisfied also for different centralities. For different projectiles and targets an approximate scaling is also satisfied although in this case some differences occur. The departure of scaling for  $\tau > 1$  follows the expected hierarchy in jet quenching, namely the suppression is larger for larger participant nuclei.

## Acknowledgements

We thank L. McLerran, N. Armesto and C. Salgado for usefull discussions. This work was supported by the Ministerio de Economía y Competitividad of Spain under the project FPA 2011-22776, by the Spanish Consolider CPAN project and by Xunta de Galicia.

## References

## References

- [1] L. McLerran and M. Praszalowicz, Acta Phys. Polon. **B41**, arXiv:1006.4293v2 [hep-ph], 1917 (2010) and Acta Phys. Polon. **B42**, 99 (2011), arXiv:1011.3403v3 [hep-ph].
- [2] M. Praszalowicz, Phys. Rev. Lett. **106**, 142002 (2011), arXiv:1101.0585v3 [hep-ph].
- [3] I. Bautista, J. Guilherme Milhano, C. Pajares and J. Dias de Deus, Phys. Lett. B **715**, 230 (2012), arXiv:1204.1457v1 [nucl-th].
- [4] I. Bautista, C. Pajares, J. Guilherme Milhano and J. Dias de Deus, Phys. Rev. C **86**, 034909 (2012), arXiv:1206.6737v1 [nucl-th].
- [5] CMS Collaboration (V. Khachatryan *et al.*), JHEP **1002** 041 (2010), arXiv:1002.0621v2 [hep-ex], Phys. Rev. Lett. **105** 022002 (2010), arXiv:1005.3299v2 [hep-ex] and JHEP **1101** 079 (2010), arXiv:1011.5531v1 [hep-ex].
- [6] ALICE Collaboration (K. Aamodt *et al.*), Phys. Rev. Lett. **105** 252301 (2010), arXiv:1011.3916 [nucl-ex] and Phys. Rev. Lett. **106** 032301 (2011), arXiv:1012.1657 [nucl-ex].
- [7] ATLAS Collaboration (G. Aad *et al.*), Phys. Lett. B **688** 21 (2010), arXiv:1003.3124v2 [hep-ex].
- [8] PHOBOS Collaboration (B.B. Back *et al.*), Phys. Rev. Lett. **94** 082304 (2005), arXiv:nucl-ex/0405003, PHOBOS Collaboration (B.B. Back *et al.*), Phys. Lett. B **578** 297 (2004), arXiv:nucl-ex/0302015v1.
- [9] PHOBOS Collaboration (B. Alver *et al.*), Phys. Rev. Lett. **96** 212301 (2006), arXiv:nucl-ex/0512016v2.
- [10] ALICE Collaboration (B. Abelev *et al.*), arXiv:1208.2711 [hep-ex].
- [11] ALICE Collaboration (B. Abelev *et al.*), arXiv:1210.4520 [nucl-ex].
- [12] ALICE Collaboration (B. Abelev *et al.*), arXiv:1210.3615 [nucl-ex].
- [13] ALICE Collaboration (B. Abelev *et al.*), arXiv:1205.3963 [hep-ex].
- [14] A. Ortiz Ph-Tesis Universidad Nacional Autónoma de México (2011).
- [15] L. McLerran and R. Venugopalan, Phys. Rev. D **49**, 2233 (1994), arXiv:hep-ph/9309289, Phys. Rev. D **49**, 3352 (1994), arXiv:hep-ph/9311205.
- [16] J. Schaffner-Bielich, D. Kharzeev, L. McLerran and R. Venugopalan, Nucl. Phys. A **705**, 494 (2002), arXiv:nucl-th/0108048.
- [17] J. Dias de Deus, E. G. Ferreira, C. Pajares and R. Ugoccioni, Eur. Phys. J. C **40**, 229 (2005), arXiv:hep-ph/0304068.
- [18] C. Pajares, Eur. Phys. J. C **43**, 9 (2005), arXiv:hep-ph/0501125.
- [19] J. Dias de Deus and C. Pajares, Phys. Lett. B **695** 211 (2011), arXiv:1011.1099 [hep-ph].